CHEMMEDCHEM

DOI: 10.1002/cmdc.200800012

# Dipeptide Derivatives of AZT: Synthesis, Chemical Stability, Activation in Human Plasma, hPEPT1 Affinity, and Antiviral Activity

Cledir Santos,[b] José Morais,[a] Luís Gouveia,[a] Erik de Clercq,[c] Christophe Pannecouque,[c] Carsten Uhd Nielsen,[d] Bente Steffansen,[d] Rui Moreira,*[a] and Paula Gomes*[b]

*5′-O-Dipeptide ester prodrugs of antiviral zidovudine (AZT) were designed to target the human intestinal oligopeptide transporter, hPEPT1, and were evaluated for their stability at pH 7.4 in buffer and in human plasma, affinity toward hPEPT1, cytotoxicity, and antiretroviral activity. The dipeptide esters of AZT undergo cyclization in buffer at pH 7.4 to release the parent drug at a rate that depends on the size of the side chains of the peptide carrier; the prodrug is considerably more stable if bulky β-branched amino acids such as Ile and Val are present, particularly as C-terminal residues. Incubation in human plasma showed that most of the dipeptide esters of AZT release the parent drug through two aminopeptidase-mediated pathways: 1) stepwise cleavage of each of the amino acids and 2) direct cleavage of the dipeptide–drug ester bond. However, the plasma hydrolysis of Gly-Gly-AZT and Phe-Gly-AZT showed only direct cleavage of the dipeptide–drug ester bond. Substrate half-lives in plasma were again remarkably high when hydrophobic β-branched amino acids (Val, Ile) were present. The esters were also good substrates for the intestinal oligopeptide transporter hPEPT1 in vitro, with Val-Gly-AZT and Val-Ala-AZT presenting the highest affinity toward the transporter ($IC_{50}$: 0.20 and 0.15 mM, respectively). The AZT dipeptide esters were assayed against the IIIB and ROD strains of HIV, and their cytotoxicity was evaluated in MT-4 cells. The selectivity index of the prodrugs was two- to threefold higher than that of AZT for all compounds analyzed. These results point to the potential of dipeptide-based carriers for the development of effective antiviral drug-delivery systems. Val-Ala-AZT appears to combine chemical stability with good affinity for the hPEPT1 transporter and an improved cytotoxicity/antiretroviral index relative to AZT.*

## Introduction

The human immunodeficiency virus (HIV), the etiological agent of acquired immunodeficiency syndrome (AIDS), is one of the most important global health problems. In 2007, the estimated number of people living infected with the virus worldwide was 33.2 million.[1] AZT (3′-azido-3′-deoxythymidine, zidovudine, Retrovir; **1**, Figure 1) was the first 2′,3′-dideoxynucleoside (ddN) approved by the US Food and Drug Administration (FDA) for the treatment of patients suffering from AIDS.[1–5] The mechanism of action of AZT involves its conversion into the corresponding 5′-*O*-triphosphate, which inhibits the replication of the virus by competitive inhibition of the viral reverse transcriptase (RT) and by incorporation and subsequent chain termination of the growing viral DNA strand.[6] Despite the development of additional RT inhibitors and agents that block other crucial steps in viral infection and replication, AZT is still the most used anti-HIV agent. However, administration of AZT is frequently associated with a significant dose-dependent toxicity, particularly destruction of bone marrow cells, myopathy, and hepatic abnormalities.[7] In addition, the short half-life

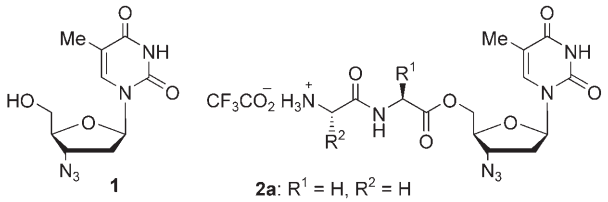

**1**

**2a**: $R^1$ = H, $R^2$ = H
**2b**: $R^1$ = *i*Pr, $R^2$ = H
**2c**: $R^1$ = $CH_2Ph$, $R^2$ = H
**2d**: $R^1$ = H, $R^2$ = *i*Pr
**2e**: $R^1$ = Me, $R^2$ = *i*Pr
**2f**: $R^1$ = $R^2$ = *i*Pr
**2g**: $R^1$ = *s*Bu, $R^2$ = *i*Pr
**2h**: $R^1$ = H, $R^2$ = $CH_2Ph$

**Figure 1.** Structure of AZT (**1**) and its dipeptide prodrugs **2**.

[a] *Prof. Dr. J. Morais, Dr. L. Gouveia, Prof. Dr. R. Moreira*
*iMed.UL, Faculdade de Farmácia, Universidade de Lisboa*
*Av. Prof. Gama Pinto, 1649-003 Lisboa (Portugal)*
*Fax: (+351) 21-794-6470*
*E-mail: rmoreira@ff.ul.pt*

[b] *Dr. C. Santos, Prof. Dr. P. Gomes*
*CIQUP, Departamento de Química, Faculdade de Ciências*
*Universidade do Porto, R. Campo Alegre 687, 4169-007 Porto (Portugal)*
*Fax: (+351) 22-040-2659*
*E-mail: pgomes@fc.up.pt*

[c] *Prof. Dr. E. de Clercq, Dr. C. Pannecouque*
*Rega Institute for Medical Research, Katholieke Universiteit Leuven*
*Minderbroedersstraat 10, 3000 Leuven (Belgium)*

[d] *Dr. C. U. Nielsen, Prof. Dr. B. Steffansen*
*Department of Pharmaceutics and Analytical Chemistry*
*The Faculty of Pharmaceutical Sciences, University of Copenhagen*
*Universitetsparken 2, 2100 Copenhagen (Denmark)*

Supporting information for this article is available on the WWW under http://www.chemmedchem.org or from the author.

  

(~1 h) of AZT in human plasma requires frequent administration to maintain therapeutic drug concentrations. Moreover, only 35 to 70% of the AZT plasma concentration is found in the cerebrospinal fluid (CSF) even at high doses.[8] The entry of AZT into brain tissue from the CSF is not sufficient to effectively suppress viral replication in the brain, thus limiting its clinical usefulness.[9]

The prodrug strategy has been widely used in attempts to deliver AZT intracellularly, to improve anti-HIV efficacy, to decrease bone marrow toxicity, to increase plasma half-life and lipophilicity, and to improve delivery to the brain.[10–23] For example, L-amino acid-5′-*O*-AZT ester prodrugs, designed to enhance the absorption of the parent drug via an amino acid transport system,[13,24,25] were reported to display less cytotoxicity than AZT. These esters of AZT were susceptible to the action of plasma esterases with half-lives of 20-70 min, except for the 5′-*O*-isoleucinyl derivative which did not undergo enzymatic hydrolysis for up to 4 h,[13] suggesting that the slow release of AZT from prodrugs may be related to the observed decrease in toxicity. When studying the mechanism of absorption of the 5′-*O*-valyl ester of AZT using the rat perfusion model, Amidon and co-workers found that the intestine was threefold more permeable to the prodrug than to AZT. Competitive inhibition studies in rats and in Chinese hamster ovarian (CHO) cells transfected with the human $H^+$/peptide cotransporter, hPEPT1, showed that the membrane transport of Val-AZT was mediated predominantly by hPEPT1, even though this compound did not contain a peptide bond. The 50% inhibition concentration ($IC_{50}$) value for Val-AZT was lower than for cephradine and enalapril, which are substrates for the peptide transporter.[26] Val-AZT also exhibited threefold higher uptake in Caco-2/hPEPT1 cells than AZT and similar studies have demonstrated that the analogous L-valyl derivative of acyclovir also displayed enhanced oral absorption due to its specific recognition by the hPEPT1 transporter. These findings were the basis for selecting 5′-amino acid esters of other antiviral nucleosides to target the intestinal hPEPT1 peptide transporter as a strategy to improve oral bioavailability. More recently, Mitra and co-workers developed dipeptide esters of acyclovir,[27,28] gancyclovir[29] and saquinavir[30,31] to improve the ocular and intestinal bioavailability of these drugs. To the best of our knowledge, dipeptide carriers have not been so far employed for AZT. In view of this, we set out to prepare and study a family of eight dipeptide esters of AZT, **2** (Figure 1), as substrates for the hPEPT1 transporter. Compounds **2** were designed taking into account the known structural requirements for molecular recognition by the peptide transporter, that is, preference for 1) the natural L,L-dipeptide skeleton, 2) a free amino group in the N-terminal, and 3) uncharged hydrophobic side-chains. To obtain structure–reactivity information, Gly, Ala, Phe, Val, and Ile residues covering a wide range of stereoelectronic properties and lipophilicity were selected. We now report the synthesis of dipeptide esters **2**, their stability and degradation pathways in pH 7.4 buffer and in human plasma, in vitro activity against HIV-1 ($III_B$) and HIV-2 (ROD) and in vitro recognition by the hPEPT1 transporter.

## Results and Discussion

### Chemistry

The synthetic pathway to the AZT prodrugs is illustrated in Scheme 1 and was based on stepwise introduction of the amino acid residues. AZT was firstly reacted with the appropriate $N^{\alpha}$-*tert*-butyloxycarbonyl-protected amino acid ($BocAA^1OH$) using *O*-(benzotriazol-1-yl)-*N*,*N*,*N*′,*N*′-tetramethyluronium tetrafluoroborate (TBTU) as coupling agent in the presence of *N*-ethyl-*N*,*N*-diisopropylamine (DIEA). The corresponding $N^{\alpha}$-Boc-protected amino acid esters **3a**–**e** were isolated, Boc removed with trifluoroacetic acid (TFA) and the resulting trifluoroacetates **4a**–**e** were then reacted with the second $N^{\alpha}$-Boc-protected amino acid ($BocAA^2OH$) to yield the protected dipeptide esters **5a**–**h** that were converted into the final products (compounds **2a**–**h**; Figure 1) again with TFA.[32,33]

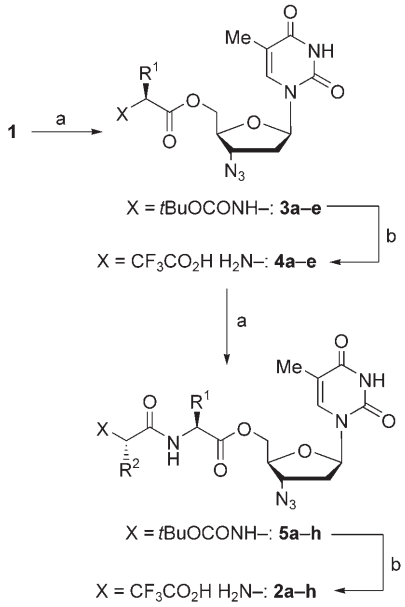


**Scheme 1.** Synthesis of AZT 5′-*O*-dipeptide esters **2a**–**h**: a) $BocAA^1OH$ or $BocAA^2OH$ (1 equiv), TBTU (1 equiv), DIEA (2 or 3 equiv), $CH_2Cl_2$, 0 °C (2 h) → room temperature (70 h); b) TFA (40% in $CH_2Cl_2$), room temperature, 30 min.

### Chemical stability

The AZT esters **2a**–**h** were incubated in pH 7.4 phosphate isotonic buffer at 37 °C and reaction progress was monitored by high-performance liquid chromatography (HPLC) and the pseudo-first-order rate constants, $k_{obs}$, thus determined are presented in Table 1. HPLC quantitative analysis of degradation products showed that AZT was released with concomitant formation of diketopiperazines (DKPs) and is consistent with the expected intramolecular acyl transfer reaction (compare with Scheme 2) that has been reported as the major degradation pathway for simple dipeptide alkyl and aryl esters.[34–36] Compounds **2a**–**h** decompose to AZT in pH 7.4 buffer with half-

  

**Table 1.** Kinetic data for the hydrolysis of compounds **2** in phosphate buffer (pH 7.4) and in human plasma at 37 °C.

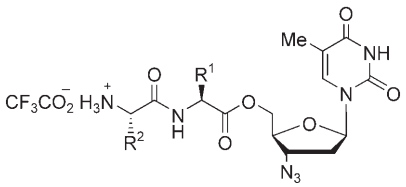

| Compound | $R^1$ | $R^2$ | Buffer | Human plasma | | | |
|---|---|---|---|---|---|---|---|
| | | | $10^4 k_{obs}$ [$s^{-1}$] | $10^4 k_{obs}$ [$s^{-1}$][a] | $10^4 k_{1,2}$ [$s^{-1}$] | $10^4 k_{1,3}$ [$s^{-1}$] | $10^4 k_{2,3}$ [$s^{-1}$] |
| **2a**, Gly-Gly-AZT | H | H | 3.91 | 23.0[b] | 0 | 23.0 | – |
| **2b**, Gly-Val-AZT | *i*Pr | H | 0.110 | 2.51 | 1.37 | 0.837 | 0.619 |
| **2c**, Gly-Phe-AZT | $CH_2Ph$ | H | 2.02 | 27.5 | 8.30 | 20.9 | 5.12 |
| **2d**, Val-Gly-AZT | H | *i*Pr | 0.578 | 4.62 | 0.367 | 4.58 | 6.98 |
| **2e**, Val-Ala-AZT | Me | *i*Pr | 0.561 | 7.29 | 3.07 | 5.62 | 9.76 |
| **2f**, Val-Val-AZT | *i*Pr | *i*Pr | 0.0207 | 1.48 | 0.989 | 0.223 | 0.740 |
| **2g**, Val-Ile-AZT | *s*Bu | *i*Pr | 0.0167 | 1.12 | 0.847 | 0.349 | 0.358 |
| **2h**, Phe-Gly-AZT | H | $CH_2Ph$ | 1.28 | 7.90[b] | 0 | 7.90 | – |

[a] Pseudo-first-order rate constants for the disappearance of dipeptide substrates **2**. [b] Direct release of AZT (no intermediate aminoacyl-AZT derivatives **4** detected).

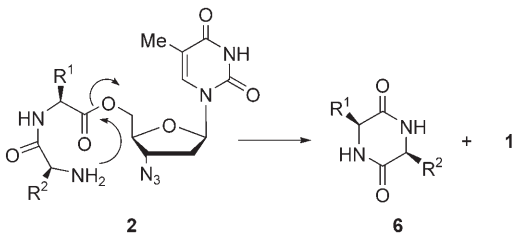

**Scheme 2.** AZT release through intramolecular cyclization of a dipeptide prodrug **2** in aqueous buffers.

lives ranging from 30 min to 115 h (Table 1). Stability of dipeptide esters **2** is dependent on the pH, increasing significantly as pH decreases (data not shown). For example, Val-Val-AZT, **2f**, showed no measurable degradation after incubation for five days in pH 4.0 buffer at 37 °C.

The rate of AZT release from **2** depends on the size of the side chains of the peptide carrier, the prodrug being considerably more stable when bulky β-branched amino acids (i.e. Ile and Val) are present as C-terminal residues. For example, the order of half-lives for the Gly-AA[1]-AZT series is Gly-Gly, **2a** < Gly-Phe, **2c** ≪ Gly-Val, **2b**, with **2b** being ~35-fold less reactive than **2a**. Similarly, for the Val-AA[1]-AZT series, Val-Gly, **2d** < Val-Ala, **2e** ≪ Val-Val, **2f** < Val-Ile, **2g**, with **2f** being ~30-fold less reactive than **2d**. The effect of a β-branched amino acid in the N-terminus of the dipeptide carrier on reactivity is smaller: for example, Gly-Val-AZT, **2b**, is only fivefold more reactive than Val-Val-AZT, **2f**. Interestingly, the same difference in reactivity was observed between the Gly-Val and Val-Val dipeptide esters of acyclovir and saquinavir at pH 7.4 and 7.2, respectively. Overall, these results suggest that steric hindrance at the C-terminus of the dipeptide backbone is the major factor affecting the rate of cyclization.[37]

### Hydrolysis in human plasma

Dipeptide esters **2** were incubated at 37 °C in 80% human plasma and their degradation monitored by HPLC. The degradation of the esters displayed first-order kinetics for three to four substrate half-lives. Detailed quantitative analysis revealed that compounds **2b**–**g** hydrolyze with formation of the corresponding amino acid esters **4** as reaction intermediates, while **2a** and **2h** release directly the parent drug in the conditions used. In all cases, formation of AZT was quantitative. These results suggest that the pathway for enzymatic degradation of esters **2** to the parent drug occurs via 1) stepwise removal of the amino acid residues and 2) direct cleavage of the dipeptide carrier (Scheme 3), depending on the amino acid sequence. An example of product analysis is presented in Figure 2 for the hydrolysis of Val-Ala-AZT, **2e**, where the solid lines represent the best computer fit to the experimental data of a model represented by Equations (1)–(3). Additional examples of time pro-

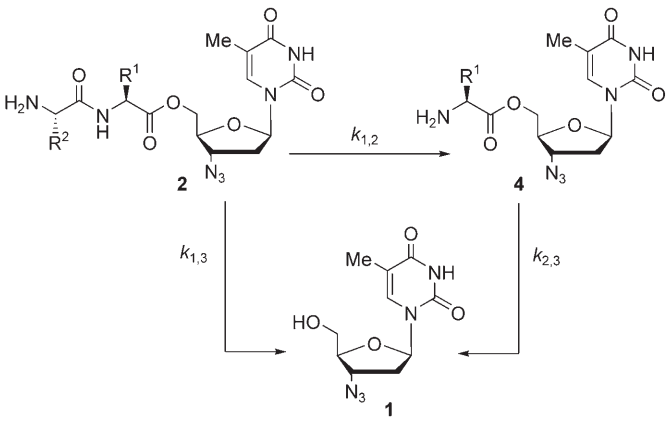

**Scheme 3.** Pathways observed for AZT release from dipeptide esters **2** in human plasma.

  

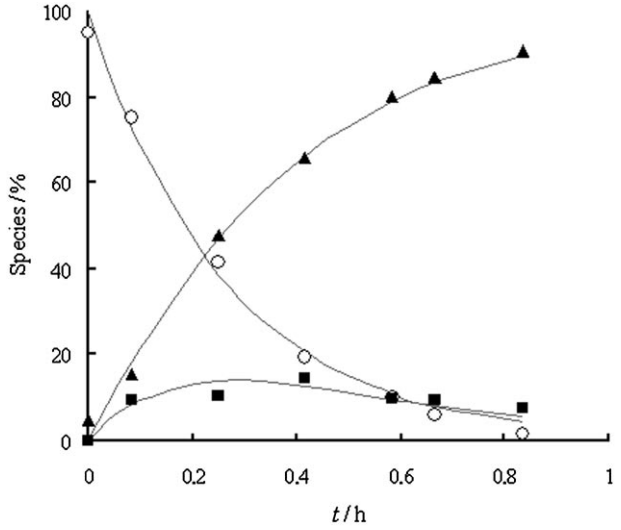


**Figure 2.** Time profile for the decomposition of **2e** (○) into **4b** (■) and AZT (▲) in 80% human plasma at pH 7.4 and 37 °C; solid lines represent the best fit of experimental data to the reaction model depicted in Scheme 3.

files for the decomposition of compounds **2** in human plasma are supplied as Supporting Information.

$$C_{1,t} = C_{1,0}\, e^{-(k_{1,2}+k_{1,3})\,t} \quad (1)$$

$$C_{2,t} = C_{1,0}\,\frac{k_{1,2}}{k_{2,3}-k_{1,2}-k_{1,3}}\left(e^{-(k_{1,2}+k_{1,3})\,t}-e^{-k_{2,3}\,t}\right) \quad (2)$$

$$C_{3,t} = C_{1,0}\left[\left(\frac{k_{1,2}\,k_{2,3}-k_{1,3}\,(k_{1,2}+k_{1,3}-k_{2,3})}{k_{1,2}+k_{1,3}}\,e^{-(k_{1,2}+k_{1,3})\,t}-k_{1,2}\,e^{-k_{2,3}\,t}\right)\Big/ (k_{1,2}+k_{1,3}-k_{2,3})+\frac{k_{1,2}\,k_{2,3}+k_{1,3}\,k_{2,3}}{(k_{1,2}+k_{1,3})\,k_{2,3}}\right] \quad (3)$$

In Equations (1)–(3), $C_1$ stands for concentration of the dipeptide ester substrate **2**, $C_2$ is the concentration of the intermediate amino acid ester **4** and $C_3$ is the concentration of AZT, $k_{1,2}$ is the first-order rate constant for the loss of the terminal amino acid, $k_{1,3}$ is the first-order rate constant for the loss of the dipeptide carrier and $k_{2,3}$ is the first-order rate constant for the hydrolysis of the amino acid intermediate **4**. The $k_{1,2}$, $k_{1,3}$ and $k_{2,3}$ values derived from the time-courses for substrates **2b**–**g** and their hydrolysis products are presented in Table 1. Further support for the degradation pathway depicted in Scheme 3 comes from the good agreement between the calculated, $k_{2,3}$, and the experimentally determined first-order rate constants, $k_{obs}$, for the plasma-catalyzed hydrolysis of amino acid ester intermediates **4a**–**e** (**4a**, Gly-AZT, $6.85\times10^{-4}\ s^{-1}$; **4b**, Ala-AZT, $8.99\times10^{-4}\ s^{-1}$; **4c**, Val-AZT, $6.25\times10^{-5}\ s^{-1}$; **4d**, Ile-AZT, $3.24\times10^{-5}\ s^{-1}$; **4e**, Phe-AZT, $5.10\times10^{-4}\ s^{-1}$). Moreover, the $k_{obs}$ values for compounds **4b**–**g** are also in good agreement with the sum of $k_{1,2}$ and $k_{1,3}$ values calculated from fitting Equations (1)–(3) to the experimental data. In contrast to **2b**–**g**, substrates **2a** and **2h** released the parent drug exclusively through direct cleavage of the dipeptide carrier, that is, with $k_{1,2}=0$. As shown in Table 1, these were also the two substrates that most rapidly degraded to yield free AZT. Interestingly, direct release of Gly-Gly has also been reported for the hydrolysis of the Gly-Gly benzyl ester in 80% human plasma.[35] The high reactivity shown by **2a** ($t_{1/2}\sim5$ min) correlates with experimental observations made in the course of the hPEPT1 affinity assays (see the following section).

The experimental observations for the degradation of **2** in human plasma are consistent with substrate enzymatic hydrolysis promoted by plasmatic amino- and diaminopeptidases, in agreement with previous findings by Jensen et al.[35] and Majumdar et al.[38] while studying di-/tripeptide esters of benzyl alcohol and the Val-Val ester of acyclovir, respectively. Dipeptide esters **2** are ~6 to 70-fold more susceptible to plasma hydrolysis than to chemical degradation in pH 7.4 buffer. Nevertheless, AZT release from **2** in human plasma is still very slow for substrates possessing two bulky β-branched amino acids, such as **2f** (Val-Val-AZT) and **2g** (Val-Ile-AZT). It is noteworthy that amino acid hydrophobicity is not enough to assure slow release of AZT, as the phenylalanine dipeptide (**2c**, **2h**) and amino acid (**2e**) esters of AZT were clearly less stable than their Val and Ile counterparts (Table 1). This is reinforced by previous findings from Yang et al. who described the phenylalanine ester of acyclovir (the counterpart of **4e**) to be highly susceptible to plasma enzymes, with an in vitro half-life of 1.3 min.[39] Thus, amino acid β-branching seems to be a key factor to induce slow release of the parent drug.

### Affinity of compounds 2 for hPEPT1 in Caco-2 cell monolayers

The affinity of dipeptide esters **2** for hPEPT1 was determined by displacement studies of [$^{14}$C]glycylsarcosine ([$^{14}$C]GlySar) in filter-grown Caco-2 cell monolayers, as described in the Experimental Section. Substrate stability under conditions employed in the uptake assays investigated by HPLC-UV showed that all compounds **2** were stable, with the exception of the glycylglycine derivative **2a**. The inhibition data for **2a**–**h** are presented as $IC_{50}$ values in Table 2. All compounds presented $IC_{50,hPEPT1}$ values under 10 mM, which is below the value reported for cephradine in CHO/hPEPT1 cells ($15\pm2$ mM),[26] except **2a**, which showed very weak affinity for hPEPT1, and **2b**, with a $IC_{50,hPEPT1}$ value of 16.8 mM.

**Table 2.** In vitro affinities of compounds **2a**–**h** for the intestinal oligopeptide transporter hPEPT1 in Caco-2 cell monolayers.

| Compound | log $P$[a] | $IC_{50,hPEPT1}$ [mM][b] |
|---|---|---|
| **2a** | −0.36 | >1000 |
| **2b** | 0.34 | 16.8±0.9 |
| **2c** | 1.04 | 7.2±1 |
| **2d** | 0.28 | 0.20±0.01 |
| **2e** | 0.63 | 0.15±0.01 |
| **2f** | 1.17 | 6.0±1 |
| **2g** | 1.58 | 8.8±0.8 |
| **2h** | 1.05 | 9.0±0.7 |

[a] Obtained using ALOGPS 2.1 (available at VCCLAB, Virtual Computational Chemistry Laboratory: http://www.vcclab.org). [b] Concentration required to decrease apical uptake of [$^{14}$C]Gly-Sar by 50%.

  

Inspection of Table 2 shows that compounds having valine as N-terminal amino acid generally displayed the highest affinities for hPEPT1 (i.e. Val-Gly-AZT, **2d**, Val-Ala-AZT, **2e** and Val-Val-AZT, **2f**), whereas the lowest affinities were observed for substrates having glycine as the N-terminal amino acid (i.e. Gly-Gly-AZT, **2a** and Gly-Val-AZT, **2b**). These results suggest that valine as the N-terminal residue of the dipeptide carrier is a major structural requirement for molecular recognition of compounds **2** by hPEPT1 and are consistent with those obtained for dipeptide and amino acid derivatives of other antiviral agents and with the hypothesis that valine might represent the optimal combination of chain length and β-branching for intestinal absorption.[40] For example, Jain et al. found that the Val-Val ester of saquinavir (Val-Val-SQV) exhibits higher absorption rate constant and intestinal permeability in rat jejunum than its Gly-Val counterpart.[31] The affinity of Val-Val-SQV toward peptide transporters expressed in MDCKII-MDR1 cells is also higher than that of Gly-Val-SQV.[30] In the present study, Val-Val-AZT **2f** also exhibited good affinity for the peptide transporter, being ranked third within the series studied. Similarly, Amidon and co-workers reported a clearly higher affinity of Val-acyclovir toward hPEPT1 relative to that of Gly-acyclovir under identical conditions.[26]

The lack of a clear correlation between $\log(1/IC_{50,hPEPT1})$ and $\log P$ presented in Figure 3, suggests that binding of prodrugs **2** to the peptide transporter does not require lipophilic dipeptidic carriers. This result contrasts with that obtained for amino acid prodrugs of the antiviral agent 2-bromo-5,6-dichloro-1-(β-D-ribofuranosyl)benzimidazole that showed a marked increase in the affinity of the prodrug for hPEPT1 transporter with the lipophilicity of the amino acid derivative.[41] However, if the sub-set Gly-AA-AZT, **2a–c**, is analyzed, then the order of Gly-Sar uptake inhibition by AA is Phe > Val ≫ Gly. This is consistent with the order of lipophilicity of AA ($\pi_{Bz}=2.6$; $\pi_{iPr}=1.3$; $\pi_{H}=0.0$) and indicates that contribution of dipeptide lipophilicity to the binding properties of prodrugs **2** cannot be entirely ruled out. A similar result was reported for the inhibition of Gly-AA dipeptides on the Gly-Sar uptake by PEPT1 in human intestinal Caco-2 cells.[42] This is further confirmed by the observation that the affinities of compounds with identical $\log P$ values do not differ significantly (e.g. Gly-Phe-AZT, **2c**, and Phe-Gly-AZT, **2h**; Table 2). For the sub-set Val-AA-AZT, **2d–g**, the order of Gly-Sar uptake inhibition by AA is Ala > Gly > Val > Leu, which suggests that steric hindrance exerted by AA might affect affinity toward hPEPT1 when a β-branched amino acid is present at the N-terminus of the dipeptide backbone.

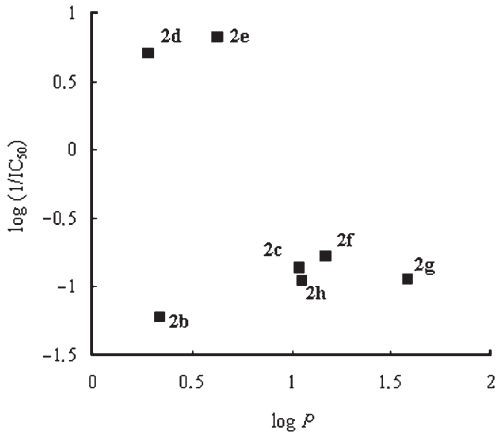


**Figure 3.** Plot of $\log(1/IC_{50,hPEPT1})$ versus $\log P$ for AZT dipeptide esters **2b–h**. The $\log P$ values were obtained using ALOGPS 2.1, available at VCCLAB, Virtual Computational Chemistry Laboratory: http://www.vcclab.org.

Full saturation curves were obtained for two of the most interesting Val-AA[1]-AZT derivatives, **2d** and **2e**, and are displayed in Figure 4. The curves do not show 100% inhibition of

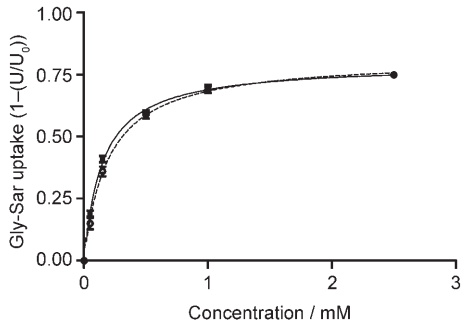


**Figure 4.** Full saturation curves for compounds **2d** (○) and **2e** (■) for hPEPT1-mediated apical Gly-Sar uptake in Caco-2 cell monolayers. Lines represent the best fit of experimental data to Equation (4).

[$^{14}$C]Gly-Sar uptake, but this might be an artifact due to a residual amount of extracellular isotope, as previously reported.[43] Both curves are almost superimposable, indicating that not only are **2d** and **2e** very good substrates for hPEPT1, but also their interactions with this transporter are remarkably similar. Any possible artifact behind this similarity, due to eventual substrate degradation in the course of uptake assays, has been ruled out by the stability study. Overall, these assays demonstrate that dipeptide esters **2** are good substrates for the intestinal hPEPT1 oligopeptide transporter, especially when valine is used as the N-terminal amino acid.

### In vitro anti-HIV and cytotoxic activity

Compounds **2a–h** were also evaluated for inhibition of the cytopathic effects of HIV-1 (IIIB) and HIV-2 (ROD) viral strains in MT-4 cells, and the results are presented in Table 3. Compound-induced cytotoxicity was also measured in MT-4 cells in parallel with the antiviral activity. As shown by the $IC_{50,HIV}$ values presented in Table 3, all dipeptide esters **2a–h** display anti-HIV activity identical to that of AZT against both HIV-1 and HIV-2.

More relevantly, the compounds showed 50% cytotoxic concentration ($CC_{50}$) values that were two- to fourfold higher than that of AZT, indicating that the AZT dipeptide esters are clearly less cytotoxic than the parent drug. Again, the Val-Ile-AZT (**2g**) derivative is the most promising compound, as it is the least cytotoxic of the series. Neither the antiviral activities nor cytotoxicities of prodrugs **2** correlated with the $\log P$ values, sug-

  

**Table 3.** Anti-retroviral activity and cytotoxicity data for AZT and its derivatives **2a–h**.

| Compd | Strain | $IC_{50,HIV}$ [nM][a] | $CC_{50}$ [μM][b] | SI[c] |
|---|---|---|---|---|
| **2a** | HIV-2 ROD | 2.9 | 15.0 | 5172 |
| | HIV-1 $III_B$ | 1.8 | | 8333 |
| **2b** | HIV-2 ROD | 4.0 | 20.0 | 5000 |
| | HIV-1 $III_B$ | 1.9 | | 10526 |
| **2c** | HIV-2 ROD | 3.0 | 14.1 | 4700 |
| | HIV-1 $III_B$ | 1.5 | | 9400 |
| **2d** | HIV-2 ROD | 2.8 | 15.6 | 5571 |
| | HIV-1 $III_B$ | 1.6 | | 9750 |
| **2e** | HIV-2 ROD | 3.2 | 19.6 | 6125 |
| | HIV-1 $III_B$ | 1.8 | | 10889 |
| **2f** | HIV-2 ROD | 3.9 | 18.1 | 4641 |
| | HIV-1 $III_B$ | 1.5 | | 12067 |
| **2g** | HIV-2 ROD | 4.0 | 19.6 | 4900 |
| | HIV-1 $III_B$ | 1.5 | | 13067 |
| **2h** | HIV-2 ROD | 2.3 | 14.4 | 6261 |
| | HIV-1 $III_B$ | 1.7 | | 8471 |
| AZT | HIV-2 ROD | 3.7 | 8.46 | 2286 |
| | HIV-1 $III_B$ | 1.9 | | 4453 |

[a] 50% inhibitory concentration, or concentration required to inhibit the viability of HIV-infected cells by 50% (average values from at least two independent assays). [b] 50% cytotoxic concentration, or concentration required to inhibit the viability of mock-infected cells by 50% (average values from at least two independent assays). [c] $SI = CC_{50}/IC_{50,HIV}$.

gesting that lipophilicity might not have a significant role in their diffusion into the cells and/or in the intracellular delivery of AZT.

Prodrugs **2a–h** are more selective than AZT, as their cytotoxicities (given by $CC_{50}$ values) are generally lower than that of the parent drug, while their anti-HIV activities (given by $IC_{50,HIV}$ values) are identical to that of AZT. This can be easily illustrated by a selectivity index (SI) associated to each compound **2a–h**, being $SI = CC_{50}/IC_{50,HIV}$ (Table 3). Thus, the data in Table 3 show that esters **2a–h** are two- to threefold more selective than the parent drug. An interesting observation is that the most selective AZT prodrugs contain a Val residue either at the N-terminus (**2d–g**) or C-terminus (**2b**) of the peptide carrier. A similar decrease in cytotoxicity for amino acid esters of AZT, as compared with the parent drug, has been also described by Aggarwal et al.[13] One of the least cytotoxic esters of the set studied by these authors was the Ile ester of AZT, which agrees with the fact that the least cytotoxic ester from Table 3 is **2g**, i.e., the dipeptide ester that also contains Ile directly bound to AZT. However, at present we cannot exclude the possibility that the released amino acid and dipeptides may have some effect on decreasing the toxicity of AZT.

## Conclusions

5′-*O*-Dipeptide ester derivatives of AZT, **2**, are quantitatively hydrolyzed to the parent drug in pH 7.4 buffer and in human plasma. Prodrugs **2** bearing β-branched amino acids, such as valine, at N-terminus of the dipeptide carrier exhibit high affinities toward the intestinal oligopeptide transporter hPEPT1. These compounds are suggested to be activated by plasma amino- and diaminopeptidases to slowly and quantitatively release the parent anti-HIV drug, with the advantage of being less cytotoxic than the parent drug. Overall, the results show that, with correct tailoring of the dipeptide moiety, dipeptide esters of AZT may represent a viable way to minimize some of the problems associated with AZT-based therapies, such as low oral bioavailability and toxicity. Such an approach would allow the re-introduction of AZT, through suitable derivatives as prodrugs, as a reference agent for the treatment of AIDS.

## Experimental Section

**Materials.** Boc-amino acids and TBTU were obtained from Bachem, and solvents were all of p.a. quality from Merck and were dried over pre-activated 3 Å molecular sieves prior to use. All remaining reactants were from Sigma–Aldrich. Silica gel 60 plates (Merck $F_{254}$) were used for thin-layer chromatography. NMR spectra were acquired on a Bruker AMX 300 spectrometer from solutions of the compounds in hexadeuterated dimethyl sulfoxide ([$D_6$]DMSO) having tetramethylsilane (TMS) as internal reference: $^1H$ and $^{13}C$ chemical shifts are given in parts per million (ppm) and proton–proton coupling constants in Hertz (Hz); $^1H$ NMR peak multiplicity is indicated by br s (broad singlet), s (singlet), d (doublet), dd (double doublet), t (triplet), q (quartet), m (unresolved multiplet). MS data were acquired by either the matrix-assisted laser desorption ionization time-of-flight (MALDI-ToF) or the electrospray ionization ion-trap (ESI-IT) techniques, on a Bruker Biflex II or a Finnigan LCQ DECA XP MAX spectrometer, respectively. Elemental analyses (EA) were run on a LECO CHNS-932 instrument.

**Synthesis of compounds 3a–e.** The relevant $BocAA^1OH$ (1 equiv), TBTU (1 equiv) and DIEA (2 equiv) were dissolved in $CH_2Cl_2$ at 0 °C and the mixture stirred for 10 min prior to addition of AZT (1 equiv). The mixture was stirred at 0 °C for further 2 h, then at room temperature for a further 70 h. After washing the crude mixture with 30% aqueous $KHSO_4$ and 30% aqueous $Na_2CO_3$, the organic layer was dried over anhydrous $MgSO_4$ and evaporated to dryness yielding a brownish oil that was identified as the desired product by NMR and MS (see Supporting Information).

**Preparation of trifluoroacetates 4a–e.** Each compound **3a–e** was dissolved in 40% TFA in $CH_2Cl_2$ and the reaction was allowed to reach completion (~30 min) at room temperature. The target trifluoroacetate was precipitated with diethyl ether and isolated after centrifugation at 3300 rpm and −9 °C. Compounds **4a–e** were isolated as white hygroscopic solids (stored over anhydrous calcium chloride on a vacuum desiccator) and their structures confirmed by NMR and EA (see Supporting Information).

**Synthesis of compounds 5a–h.** Two solutions were prepared in parallel in separate flasks at 0 °C, one containing each trifluoroacetate **4a–e** (1 equiv) and DIEA (1 equiv) dissolved in $CH_2Cl_2$ and the other containing the relevant $BocAA^2OH$ (1 equiv), TBTU (1 equiv) and DIEA (2 equiv) also in $CH_2Cl_2$. After being stirred for 10 min, both solutions were mixed together and subsequent procedures were as described for compounds **3**. Compounds **5** were isolated pure, as brownish oils, and their identity confirmed by NMR and MS (see Supporting Information).

**Preparation of the target trifluoroacetates 2a–h.** The final compounds were obtained as white hygroscopic solids by acidolysis of their Boc-protected precursors **5a–h**, following the procedure described above for the preparation of trifluoroacetates **4a–e**. Their structures were confirmed by NMR and EA, as described below.

  

*O*-Glycylglycyl-3′-azido-2′,3′-dideoxythymine trifluoroacetic acid salt, **2a.** Yield, 25%; $^1$H NMR (300 MHz, [D$_6$]DMSO, 25 °C, TMS): $\delta$ = 1.80 (s, 3H, CH$_3$); 2.34–2.48 (m, 2H, CH$_2$); 3.63 (s, 2H, CH$_2$); 3.99 (m, 3H, C*H*H + CH$_2$); 4.31 (m, 2H, CH + CH); 4.51 (m, 1H, CH*H*); 6.12 (t, $^3J$(H,H) = 6.3 Hz, 1H, CH); 7.46 (s, 1H, =CH); 8.11 (brs, 3H, NH$_3^+$); 8.87 (t, $^3J$(H,H) = 5.7 Hz, 1H, NH); 11.3 ppm (s, 1H, NH). $^{13}$C NMR (75.4 MHz, [D$_6$]DMSO, 25 °C, TMS): $\delta$ = 12.05 (CH$_3$); 35.39 (CH$_2$); 40.48 (CH$_2$); 59.82 (CH); 63.87 (CH$_2$); 80.40 (CH); 83.58 (CH); 109.92 (C=); 136.09 (=CH); 150.31 (CO); 163.60 (CO); 166.59 (CO); 169.20 ppm (CO). $C_{16}H_{20}F_3N_7O_8\cdot 2H_2O$ (531.16 g mol$^{-1}$): N, 18.46; C, 36.18; H, 4.55%; Found: N, 18.80; C, 36.33; H, 4.33%.

*O*-Glycylvalyl-3′-azido-2′,3′-dideoxythymine trifluoroacetic acid salt, **2b**. Yield, 73%; $^1$H NMR (300 MHz, [D$_6$]DMSO, 25 °C, TMS): $\delta$ = 0.90 (d, $^3J$(H,H) = 6.9 Hz, 6H, 2×CH$_3$); 1.81 (s, 3H, CH$_3$); 2.11–2.35 (m, 2H, CH$_2$); 2.54 (m, 1H, CH); 3.66 (s, 2H, CH$_2$); 4.00 (m, 1H, C*H*H); 4.32 (m, 3H, 3×CH); 4.51 (m, 1H, CH*H*); 6.12 (t, $^3J$(H,H) = 6.6 Hz, 1H, CH); 7.46 (s, 1H, =CH); 8.10 (brs, 3H, NH$_3^+$); 8.71 (d, $^3J$(H,H) = 8.1 Hz, 1H, NH); 11.4 ppm (s, 1H, NH). $^{13}$C NMR (75.4 MHz, [D$_6$]DMSO, 25 °C, TMS): $\delta$ = 12.04 (CH$_3$); 17.75 (CH$_3$); 18.78 (CH$_3$); 29.95 (CH); 35.32 (CH$_2$); 57.38 (CH); 60.09 (CH); 64.04 (CH$_2$); 80.32 (CH); 83.72 (CH); 109.89 (C=); 136.02 (=CH); 150.31 (CO); 163.59 (CO); 166.39 (CO); 170.83 ppm (CO). $C_{19}H_{26}F_3N_7O_8\cdot H_2O$ (555.20 g mol$^{-1}$): N, 17.66; C, 41.10; H, 5.08%; Found: N, 17.21; C, 40.63; H, 4.95%.

*O*-Glycylphenylalanyl-3′-azido-2′,3′-dideoxythymine trifluoroacetic acid salt, **2c**. Yield, 93%; $^1$H NMR (300 MHz, [D$_6$]DMSO, 25 °C, TMS): $\delta$ = 1.80 (s, 3H, CH$_3$); 2.34 (m, 2H, CH$_2$); 2.98 (dd, $^2J$(H,H) = 13.8 Hz, $^3J$(H,H) = 8.4 Hz, 1H, C*H*H); 3.08 (dd, $^2J$(H,H) = 13.7 Hz, $^3J$(H,H) = 5.9 Hz, 1H, CH*H*); 3.58 (s, 2H, CH$_2$); 3.96 (m, 1H, CH*H*); 4.26 (m, 3H, 3×CH); 4.61 (m, 1H, CH*H*); 6.11 (t, $^3J$(H,H) = 6.6 Hz, 1H, NH); 7.24 (m, 5H, ArH); 7.44 (s, 1H, =CH); 8.07 (brs, 3H, NH$_3^+$); 8.97 (d, $^3J$-(H,H) = 7.5 Hz, NH); 11.4 ppm (s, 1H, NH). $^{13}$C NMR (75.4 MHz, [D$_6$]DMSO, 25 °C, TMS): $\delta$ = 12.09 (CH$_3$); 35.48 (CH$_2$); 36.67 (CH$_2$); 53.79 (CH); 59.85 (CH); 64.20 (CH$_2$); 80.26 (CH); 83.60 (CH); 109.97 (C=); 126.74 (ArCH); 128.32 (ArCH); 129.04 (ArCH); 135.86 (ArC); 136.50 (=CH); 150.29 (CO); 163.60 (CO); 166.11 (CO); 170.75 ppm (CO). $C_{23}H_{26}F_3N_7O_8\cdot H_2O$ (603.20 g mol$^{-1}$): N, 16.25; C, 45.79; H, 4.70%; Found: N, 15.92; C, 45.34; H, 4.71%.

*O*-Valylglycyl-3′-azido-2′,3′-dideoxythymine trifluoroacetic acid salt, **2d**. Yield, 73%; $^1$H NMR (300 MHz, [D$_6$]DMSO, 25 °C, TMS): $\delta$ = 0.96 (m, 6H, 2×CH$_3$); 1.80 (s, 3H, CH$_3$); 2.09–2.35 (m, 2H, CH$_2$); 2.48 (m, 1H, CH); 3.67 (d, $^3J$(H,H) = 5.1 Hz, 1H, CH); 3.98 (m, 2H, CH$_2$); 4.06 (m, 1H, C*H*H); 4.32 (m, 2H, 2×CH); 4.48 (m, 1H, CH*H*); 6.14 (t, $^3J$-(H,H) = 6.6 Hz, 1H, CH); 7.48 (s, 1H, =CH); 8.17 (brs, 3H, NH$_3^+$); 8.93 (m, 1H, NH); 11.4 ppm (s, 1H, NH). $^{13}$C NMR (75.4 MHz, [D$_6$]DMSO, 25 °C, TMS): $\delta$ = 12.03 (CH$_3$); 17.54 (CH$_3$); 17.99 (CH$_3$); 29.74 (CH); 35.36 (CH$_2$); 40.46 (CH$_2$); 57.19 (CH); 59.91 (CH); 63.97 (CH$_2$); 80.41 (CH); 83.59 (CH); 109.89 (=C); 136.09 (=CH); 150.31 (CO); 163.58 (CO); 168.42 (CO); 169.10 ppm (CO). $C_{19}H_{26}F_3N_7O_8\cdot 2H_2O$ (573.21 g mol$^{-1}$): N, 17.10; C, 39.81; H, 5.27%; Found: N, 17.05; C, 40.19; H, 5.02%.

*O*-Valylalanyl-3′-azido-2′,3′-dideoxythymine trifluoroacetic acid salt, **2e**. Yield, 75%; $^1$H NMR (300 MHz, [D$_6$]DMSO, 25 °C, TMS): $\delta$ = 0.95 (m, 6H, 2×CH$_3$); 1.36 (d, $^3J$(H,H) = 7.5 Hz, 3H, CH$_3$); 1.80 (s, 3H, CH$_3$); 2.07–2.33 (m, 2H, CH$_2$); 2.48 (m, 1H, CH); 3.61 (d, $^3J$(H,H) = 5.1 Hz, 1H, CH); 3.97 (m, 1H, C*H*H); 4.30 (m, 2H, 2×CH); 4.38 (m, 1H, CH); 4.45 (m, 1H, CH*H*); 6.10 (t, $^3J$(H,H) = 6.6 Hz, 1H, CH); 7.47 (s, 1H, =CH); 8.14 (brs, 3H, NH$_3^+$); 8.90 (d, $^3J$(H,H) = 6.3 Hz, 1H, NH); 11.4 ppm (s, 1H, NH). $^{13}$C NMR (75.4 MHz, [D$_6$]DMSO, 25 °C, TMS): $\delta$ = 12.00 (CH$_3$); 16.65 (CH$_3$); 17.47 (CH$_3$); 18.04 (CH$_3$); 29.72 (CH$_3$); 35.28 (CH$_2$); 47.65 (CH); 57.12 (CH); 60.05 (CH); 64.11 (CH$_2$); 80.34 (CH); 83.60 (CH); 109.90 (=C); 136.03 (=CH); 150.30 (CO); 163.57 (CO); 167.72 (CO); 171.68 ppm (CO). $C_{20}H_{28}F_3N_7O_8\cdot H_2O$ (569.22 g mol$^{-1}$): N, 17.22; C, 42.20; H, 5.31%; Found: N, 17.00; C, 41.90; H, 5.31%.

*O*-Valylvalyl-3′-azido-2′,3′-dideoxythymine trifluoroacetic acid salt, **2f.** Yield, 58%; $^1$H NMR (300 MHz, [D$_6$]DMSO, 25 °C, TMS): $\delta$ = 0.94 (m, 12H, 4×CH$_3$); 1.80 (s, 3H, CH$_3$); 2.11–2.34 (m, 3H, CH + CH$_2$); 2.48 (m, 1H, CH); 3.76 (m, 1H, CH); 3.98 (m, 1H, C*H*H); 4.29 (m, 3H, 3×CH); 4.47 (m, 1H, CH*H*); 6.12 (t, $^3J$(H,H) = 6.6 Hz, 1H, CH); 7.48 (s, 1H, =CH); 8.14 (brs, 3H, NH$_3^+$); 8.66 (d, $^3J$(H,H) = 7.5 Hz, 1H, NH); 11.4 ppm (s, 1H, NH). $^{13}$C NMR (75.4 MHz, [D$_6$]DMSO, 25 °C, TMS): $\delta$ = 12.00 (CH$_3$); 17.36 (CH$_3$); 17.88 (CH$_3$); 18.16 (CH$_3$); 18.74 (CH$_3$); 29.60 (CH); 29.84 (CH); 35.20 (CH$_2$); 56.90 (CH); 57.65 (CH); 60.18 (CH); 64.11 (CH$_2$); 80.33 (CH); 83.66 (CH); 109.86 (=C); 136.04 (=CH); 150.31 (CO); 163.57 (CO); 168.37 (CO); 170.59 ppm (CO). $C_{22}H_{32}F_3N_7O_8\cdot H_2O$ (597.25 g mol$^{-1}$): N, 16.42; C, 44.24; H, 5.74%; Found: N, 16.21; C, 44.22; H, 5.87%.

*O*-Valylisoleucyl-3′-azido-2′,3′-dideoxythymine trifluoroacetic acid salt, **2g**. Yield, 38%; $^1$H NMR (300 MHz, [D$_6$]DMSO, 25 °C, TMS): $\delta$ = 0.88 (m, 12H, 4×CH$_3$); 1.23 (m, 1H, C*H*H); 1.40 (m, 1H, CH*H*); 1.80 (s, 3H, CH$_3$); 1.84 (m, 1H, CH); 2.08–2.34 (m, 2H, CH$_2$); 2.48 (m, 1H, CH); 3.72 (d, $^3J$(H,H) = 5.1 Hz, CH); 3.98 (m, 1H, C*H*H); 4.30 (m, 3H, 3×CH); 4.45 (m, 1H, CH*H*); 6.12 (t, $^3J$(H,H) = 6.6 Hz, CH); 7.47 (s, 1H, =CH); 8.08 (brs, 3H, NH$_3^+$); 8.62 ppm (m, 1H, NH); 11.4 (s, 1H, NH). $^{13}$C NMR (75.4 MHz, [D$_6$]DMSO, 25 °C, TMS): $\delta$ = 11.13 (CH$_3$); 12.00 (CH$_3$); 15.29 (CH$_3$); 17.37 (CH$_3$); 18.15 (CH$_3$); 24.53 (CH$_2$); 29.84 (CH); 35.13 (CH$_2$); 36.10 (CH); 56.65 (CH); 56.93 (CH); 60.28 (CH); 64.20 (CH$_2$); 80.33 (CH); 83.73 (CH); 109.84 (=C); 136.06 (=C); 150.31 (CO); 163.57 (CO); 168.32 (CO); 170.56 ppm (CO). $C_{23}H_{34}F_3N_7O_8\cdot 2H_2O$ (629.27 g mol$^{-1}$): N, 15.58; C, 43.89; H, 6.08%; Found: N, 15.43; C, 44.01; H, 5.93%.

*O*-Phenylalanylglycyl-3′-azido-2′,3′-dideoxythymine trifluoroacetic acid salt, **2h**. Yield, 73%; $^1$H NMR (300 MHz, [D$_6$]DMSO, 25 °C, TMS): $\delta$ = 1.80 (s, 3H, CH$_3$); 2.36–2.48 (m, 2H, CH$_2$); 2.96 (m, 1H, C*H*H); 3.13 (m, 1H, CH*H*); 4.00 (m, 3H, 3×CH); 4.09 (m, 1H, C*H*H); 4.32 (m, 2H, CH$_2$); 4.52 (m, 1H, CH*H*); 6.13 (t, $^3J$(H,H) = 6.6 Hz, 1H, CH); 7.29 (m, 5H, ArH); 7.47 (s, 1H, =CH); 8.19 (brs, 3H, NH$_3^+$); 9.00 ppm (m, 1H, NH); 11.4 (s,1H, NH). $^{13}$C NMR (75.4 MHz, [D$_6$]DMSO, 25 °C, TMS): $\delta$ = 12.05 (CH$_3$); 35.37 (CH$_2$); 36.93 (CH$_2$); 40.54 (CH$_2$); 53.24 (CH); 59.84 (CH); 63.96 (CH$_2$); 80.42 (CH); 83.61 (CH); 109.90 (=C); 127.10 (ArCH); 128.46 (ArCH); 129.46 (ArCH); 134.69 (ArC); 136.10 (=CH); 150.30 (CO); 163.59 (CO); 168.70 (CO); 169.05 ppm (CO). $C_{23}H_{26}F_3N_7O_8\cdot 1.5H_2O$ (612.52 g mol$^{-1}$): N, 16.00; C, 45.10; H, 4.27%; Found: N, 16.21; C, 44.22; H, 4.87%.

**General procedure for the monitoring of AZT release by HPLC–UV.** A solution of the compound to be assayed ($10^{-4}$ M) in aqueous buffer (pH 7.4) was kept at a constant temperature of 37.0 ± 0.1 °C; aliquots were periodically taken and immediately injected (loop of 100 μL) in the HPLC system, using a LichroCart 250–4 Lichrospher 100 RP-8 reversed-phase column (250×4 mm, 5 μm); the elution was isocratic, at varying proportions of CH$_3$CN in aqueous buffer (sodium hexanesulfonate 10 mM, sodium acetate 2.5 mM, phosphoric acid 2.5 mM; pH 6.3) and at a flow rate of 1.0 mL min$^{-1}$, with UV detection at 240 nm; AZT and the relevant diketopiperazines (DKPs) were used as standards for peak identification. The hydrolyses of prodrugs in human plasma were studied by the HPLC-UV method described above. Plasma was obtained from heparinized blood of healthy donors, pooled, and frozen at −70 °C before use. The prodrugs were incubated at an initial concentration of $10^{-4}$ M at 37 °C in human plasma diluted to 80% (*v/v*) with pH 7.4 isotonic phosphate buffer. At appropriate intervals, 30 μL

  

aliquots were added to 270 μL acetonitrile in order to quench the reaction and to eliminate proteins from the plasma. These samples were centrifuged for 5 min at 13 000 rpm and the supernatant was analyzed by HPLC for the presence of substrate, AZT, DKP and corresponding 5′-*O*-amino acid intermediate.

### Affinity for hPEPT1 in Caco-2 cells

**Materials.** Caco-2 human colon carcinoma cells were obtained from the ATCC (Rockville, MD, USA). Cell culture media and Hank's balanced salt solution (HBSS) were obtained from Life Technologies (Høje Tåstrup, Denmark). [$^{14}$C]Gly-Sar with a specific activity of 49.90 mCi mmol$^{-1}$ was purchased from New England Nuclear (Boston, MA). 2-[*N*-Morpholino]ethanesulfonic acid (MES), 2-[4-(2-hydroxyethyl)-1-piperazine]ethanesulfonic acid (HEPES), and glycylsarcosine (Gly-Sar) were purchased from Sigma–Aldrich (St. Louis, MO, USA). All analytical grade solvents used for HPLC analysis were obtained from Merck (Darmstadt, Germany), and Ultima Gold scintillation fluid was purchased from Packard (Groningen, The Netherlands). Transepithelial resistance (TEER) was measured in tissue resistance measurement chambers (Endohm) with a voltohmmeter from World Precision Instruments (Sarasota, FL, USA). The Swip KS 10 Digi shaking plate used for cell culture experiments was from Edmund Bühler (Hechingen, Germany). Caco-2 cell monolayers with a TEER higher than 200 Ω cm$^2$ were used for affinity studies. Radioactivity was counted with a Tri-Carp 2110TR liquid scintillation analyzer from Packard (Perkin–Elmer Life and Analytical Sciences, Boston, MA).

**Affinity assays.** The affinities of compounds **2b**–**h** were determined as $IC_{50}$-values by studying the inhibition of apical [$^{14}$C]Gly-Sar uptake into filter-grown 25 days old Caco-2 cell monolayers, as described previously.[44] In short, the applied buffers were HBSS supplemented with 0.05% bovine serum albumin (BSA) and 10 mM MES (pH 6.0) or 10 mM HEPES (pH 7.4). The cell monolayer was initially incubated for 15 min at 37 °C with buffers at pH 6.0 and 7.4 applied apically and basolaterally, respectively. The inhibition study was then performed by apically incubating the monolayer for 5 min at 37 °C with a mixture of 0.5 μCi [$^{14}$C]Gly-Sar and 10 mM compounds **2**. After incubation, the cells were washed three times with ice-cold HBSS, and the individual filters were removed to count the cell-associated radioactivity by liquid scintillation analysis. Full saturation curves were measured for compounds **2c** and **2d**, through similar inhibition experiments where the concentration of **2c** and **2d** ranged from 0 to 2.5 mM. The $IC_{50}$ were estimated either from the full saturation curve or from the degree of Gly-Sar inhibition observed at 10 mM compounds **2** using Michaelis–Menten-like kinetic analysis:

$$1-\frac{U}{U_0}=\frac{\left(1\left(\frac{U}{U_0}\right)\right)_{max}[I]}{IC_{50}+[I]} \quad (4)$$

where $U$ is the apical uptake of Gly-Sar, $U_0$ is the apical uptake of Gly-Sar without inhibitor, $[I]$ is the concentration of inhibitor, and $IC_{50}$ is the concentration of inhibitor required to decrease the apical uptake of [$^{14}$C]Gly-Sar by 50%. Measurements were carried out in duplicate ($N=2$) using three individual Caco-2 cell passages ($n=3$).

### Stability in 80% human plasma

**HPLC–UV analysis.** High-performance liquid chromatography (HPLC) measurements were carried out using a Waters assembly equipped with a model 600 controlled pump and a model 991 photodiode-array detector. A Rheodyne 7725 injection valve equipped with 20 μL sample loop was used. Acquisition and treatment of data were made by means of NEC for MS-DOS, version 3.30 software. The separation was performed on a Purospher, 250×4.0 mm i.d. 5 μm (Merck, Germany) analytical column, with a LiChrospher 100 RP-8 5 μm (Merck, Germany) pre-column. The solvent system used was a mixture of 78% (*v*/*v*) sodium acetate buffer (pH 6.30; 2.50 mM) (A) and 22% (*v*/*v*) acetonitrile (B) for isocratic elution of compounds **2b** and **2d**–**f**. Elution of **2a** was isocratic at 18% B, whereas for compounds **2c** and **2g**–**h** a gradient elution was carried out as follows: 0 min, 23% B; 5.0 min, 23% B; 6.0 min, 30% B; 11.0 min, 30%; 11.5 min, 23% B; 15.0 min, 23% B. Solvent flow rate was 1 mL/min for isocratic elutions and 1.5 mL min$^{-1}$ for gradient elutions. A 15 mL min$^{-1}$ nitrogen sparge was applied to remove dissolved gases. Chromatographic separation was monitored by UV detection at 265 nm. All analyses were performed at room temperature.

**Hydrolysis in human plasma.** Compounds **2** were incubated at 37 °C in human plasma (from heparinized blood of healthy donors) diluted to 80% (*v*/*v*) with pH 7.4 isotonic phosphate buffer. At appropriate intervals, aliquots were added to acetonitrile to quench the reaction and precipitate plasma proteins. These samples were centrifuged and the supernatant was analyzed by the HPLC method described above for the presence of substrate and products.

**In vitro anti-HIV assays**. The methodology of the anti-HIV assays has been previously described.[45] Briefly, MT-4 cells were infected with HIV-1 ($III_B$) and HIV-2 (ROD) at 100-fold the $CCID_{50}$ (50% cell culture infective dose) value per mL cell suspension. Then, 100 μL of the infected cell suspension were transferred to microtiter plate wells, mixed with 100 μL of the appropriate dilutions of test compounds, and further incubated at 37 °C. After 5 days of incubation of MT-4 cells, the number of viable cells was determined by a tetrazolium-based colorimetric method. The 50% inhibition concentration ($IC_{50}$) was defined as the concentration of compound required to inhibit cell viability by 50% in MT-4 cells. The cytotoxic concentration $CC_{50}$ was determined as the concentration of compound required to inhibit by 50% the number of viable cells in mock-infected MT-4 cell cultures.

## Acknowledgements

*Thanks are due to the Fundação para a Ciência e Tecnologia (Portugal) for financial support through pluriannual funding of research units CIQUP (P.G.), CECF (R.M.), and through doctoral grant SFRH/BD/9277/2002 (C.R.S.). C.R.S. and P.G. thank LAFEPE (P.E., Brazil) and Farmanguinhos (R.J., Brazil), for their kind gift of AZT. The hPEPT1 experiments were funded by the Danish Medical Research Council by project Grant no. 22-01-0310 as well as by The BioSim Network under the EU 6th Framework program.*

**Keywords:** antiviral agents · AZT · dipeptides · drug delivery · HIV · prodrugs

[1] UNAIDS, AIDS Epidemic Update, December **2007**: http://www.unaids.org/en/KnowledgeCentre/HIVData/EpiUpdate/EpiUpdArchive/2007/.

[2] "Malaria and HIV interactions and their implications for public health policy": WHO, Report of a Technical Consultation, Geneva, Switzerland, **2005**.

  

[3] M. A. Fischl, D. D. Richman, M. H. Grieco, M. S. Gottlieb, P. A. Volberding, O. L. Laskin, J. M. Leedom, J. E. Groopman, D. Mildvan, R. T. Schooley, G. G. Jackson, D. T. Durack, D. King, *N. Engl. J. Med.* **1987**, *317*, 185–191.
[4] E. De Clercq, *J. Med. Chem.* **1995**, *38*, 2491–2517.
[5] K. von der Helm, *Biol. Chem.* **1996**, *377*, 765–774.
[6] P. Mohan, *Drug Des. Rev.* **1993**, *29*, 1–17.
[7] B. A. Styrt, T. D. Piazza-Hepp, G. K. Chikami, *Antiviral Res.* **1996**, *31*, 121–135.
[8] R. W. Klecker, Jr., J. M. Collins, R. Yarchoan, R. Thomas, J. F. Jenkins, S. Broder, C. E. Meyers, *Clin. Pharmacol. Ther.* **1987**, *41*, 407–412.
[9] S. Ellison, T. Terasaki, W. M. Pardridge, *Clin. Res.* **1988**, *36*, 117 A.
[10] N. Bodor, H. H. Farag, M. E. Brewster, *Science* **1981**, *214*, 1370–1372.
[11] N. Bodor, *Drugs Future* **1981**, *6*, 165.
[12] T. Kawaguchi, K. Ishikawa, T. Seki, K. J. Juni, *Pharm. Sci.* **1990**, *79*, 531–533.
[13] S. K. Aggarwal, S. R. Gogu, S. R. S. Rangan, K. C. Agrawal, *J. Med. Chem.* **1990**, *33*, 1505–1510.
[14] C. Piantadosi, C. J. Marasco, S. L. Morris-Natschke, K. L. Meyer, F. Gumus, J. R. Surles, K. S. Ishaq, L. S. Kucera, N. Iyer, A. Wallen, S. Piantadosi, E. J. Modest, *J. Med. Chem.* **1991**, *34*, 1408–1414.
[15] K. Y. Hostetler, *PCT Int. Appl.*, WO 90/00555, January 25, **1990** [*Chem. Abst. 113*:78902s].
[16] K. Y. Hostetler, L. M. Stuhmiller, H. B. Lenting, H. van den Bosch, D. D. Richman, *J. Biol. Chem.* **1990**, *265*, 6112–6117.
[17] J. M. Steim, C. C. Neto, P. S. Sarin, D. K. Sun, R. K. Sehgal, J. G. Turcotte, *Biochem. Biophys. Res. Commun.* **1990**, *171*, 451–457.
[18] P. F. Torrence, J. Kinjo, K. Lesiak, J. Balzarini, E. De Clercq, *FEBS Lett.* **1988**, *234*, 135–140.
[19] C. K. Chu, V. S. Bhadti, K. J. Doshi, E. T. Etse, J. M. Gallo, F. D. Boudinot, R. F. Schinazi, *J. Med. Chem.* **1990**, *33*, 2188–2192.
[20] E. Palomino, D. Kessel, J. P. Horwitz, *J. Med. Chem.* **1989**, *32*, 622–625.
[21] C. McGuigan, K. G. Devine, T. J. O'Connor, A. Galpin, D. J. Jeffries, D. Kinchington, *Antiviral Chem. Chemother.* **1990**, *1*, 107–114.
[22] C. McGuigan, S. R. Nicholls, T. J. O'Connor, D. Kinchington, *Antiviral Chem. Chemother.* **1990**, *1*, 25–33.
[23] T. Yajima, K. Juni, M. Saneyoshi, T. Hasegawa, T. Kawaguchi, *Biol. Pharm. Bull.* **1998**, *21*, 272–277.
[24] R. H. Lupia, N. Ferencz, J. L. Lertora, S. K. Aggarwal, W. J. George, K. C. Agrawal, *Antimicrob. Agents Chemother.* **1993**, *37*, 818–824.
[25] B. M. Tadayoni, P. M. Friden, L. R. Walus, G. F. Musso, *Bioconjugate Chem.* **1993**, *4*, 139–145.
[26] H.-K. Han, R. L. A. de Vrueh, J. K. Rhie, K.-M. Y. Covitz, P. L. Smith, C.-P. Lee, D.-M. Oh, W. Sadee, G. Amidon, *Pharm. Res.* **1998**, *15*, 1154–1159.
[27] Y. E. Nashed, A. K. Mitra, *Spectrochim. Acta Part A Mol. Biomol. Spectrosc.* **2003**, *59*, 2033–2039.
[28] B. S. Anand, J. M. Hill, S. Dey, K. Maruyama, P. S. Bhattacharjee, M. E. Myles, Y. E. Nashed, A. K. Mitra, *Invest. Ophthalmol. Visual Sci.* **2003**, *44*, 2529–2534.
[29] S. Majumdar, Y. E. Nashed, K. Patel, R. Jain, M. Itahashi, D. M. Neumann, J. M. Hill, A. K. Mitra, *J. Ocul. Pharmacol. Ther.* **2005**, *21*, 463–474.
[30] R. Jain, S. Agarwal, S. Majumdar, X. Zhu, D. Pal, A. K. Mitra, *Int. J. Pharm.* **2005**, *303*, 8–19.
[31] R. Jain, S. Duvvuri, V. Kansara, N. S. Mandava, A. K. Mitra, *Int. J. Pharm.* **2007**, *336*, 233–240.
[32] P. Lloyd-Williams, F. Albericio, E. Giralt, *Chemical Approaches to the Synthesis of Peptides and Proteins*; CRC, Boca Raton, **1997**.
[33] C. Santos, M. L. Mateus, A. P. dos Santos, R. Moreira, E. de Oliveira, P. Gomes, *Bioorg. Med. Chem. Lett.* **2005**, *15*, 1595–1598.
[34] J. E. Purdie, N. L. Benoiton, *J. Chem. Soc. Perkin Trans. 2* **1973**, 1845–1852.
[35] E. Jensen, H. Bundgaard, *Int. J. Pharm.* **1991**, *71*, 117–125.
[36] S. W. Larsen, M. Ankersen, C. Larsen, *Eur. J. Pharm. Sci.* **2004**, *22*, 399–400.
[37] G. A. R. Y. Suaifan, M. F. Mahon, T. Arafat, M. D. Threadgill, *Tetrahedron* **2006**, *62*, 11245–11266.
[38] S. Majumdar, S. Duvvuri, A. K. Mitra, *Clin. Res. Reg. Affairs* **2004**, *21*, 67–79.
[39] C. Yang, H. Gao, A. K. Mitra, *J. Pharm. Sci.* **2001**, *90*, 617–623.
[40] L. M. Beauchamp, G. F. Orr, P. de Miranda, T. Burnette, T. A. Krenitsky, *Antiviral Chem. Chemother.* **1992**, *3*, 157–164.
[41] X. Song, B. S. Vig, P. L. Lorenzi, J. C. Drach, L. B. Townsend, G. L. Amidon, *J. Med. Chem.* **2005**, *48*, 1274–1277.
[42] H. Abe, M. Satoh, S. Miyauchi, S. Shuto, A. Matsuda, N. Kamo, *Bioconjugate Chem.* **1999**, *10*, 24–31.
[43] A. H. Eriksson, P. L. Elm, M. Begtrup, R. Nielsen, B. Steffansen, B. Brodin, *Mol. Pharm.* **2005**, *2*, 242–249.
[44] C. U. Nielsen, R. Andersen, B. Brodin, S. Frokjaer, M. Taub, B. Steffansen, *J. Controlled Release* **2001**, *76*, 129–138.
[45] R. Pauwels, J. Balzarini, M. Baba, R. Snoeck, D. Schols, P. Herdewijn, J. Desmyter, E. De Clercq, *J. Virol. Methods* **1988**, *20*, 309–321.

Received: January 18, 2008
Revised: March 4, 2008
Published online on April 3, 2008

  